J. Plasma Fusion Res. SERIES, Vol.1 (1998) 99–102

Core Fluctuations and Non-Thermal Electron Distributions at W7-AS

HÄSE Marcus, PERNREITER Walter and HARTFUSS Hans*
Max-Planck-Institut für Plasmaphysik, EURATOM Ass., 85748 Garching, Germany

(Received: 30 September 1997/Accepted: 12 January 1998)

Abstract

Two special applications of ECE radiometry at W7-AS, for measurement of temperature fluctuations and non-thermal electron distributions, are presented. In the first case correlation-radiometry is applied. The fluctuation spectra are found to be composed of two components, a diffusive and a turbulent one, with relative levels of 0.1–2%. The latter one is discussed in the frame of a turbulent mixing process. To investigate non-thermal electron energy distributions a vertical ECE observation geometry allowing for separation of both thermal and suprathermal populations and their time behaviour is used. Experimental results by variation of plasma parameters are shown and compared with simulated spectra.

Keywords:

ECE diagnostic, temperature fluctuations, turbulence, non-thermal electron distributions, suprathermal emission

1. Core Temperature Fluctuations

1.1 Characterization

Temperature fluctuation measurements are carried out in the context of turbulent transport, which is assumed to be driven at least in parts by fluctuations [9]. The sensitivity limit set by the inherent noise of an ECE-radiometer can be overcome by correlation of two separate radiometers focusing a common plasma volume [8]. Due to the demands for stationarity of the discharge during the correlation analysis only ECR heated plasmas are investigated. Typical parameters are: 2.5 T on-axis magnetic field, rotational transform $\iota = 1/3$, $P_{ECRH} = 300–800$ kW (on-axis), peaked temperature profile (T_{max} = 2.5 keV) and flat density profile ($n_{max} = 2–8 \times 10^{19}$ m^{-3}). Six radial positions on the high-field side of the core plasma ($r_{eff} = 5–10$ cm, *i.e.* $r/a = 0.3–0.6$) are observed simultaneously. The relative fluctuation spectra extend up to 50–150 kHz, with radially increasing fluctuation power. Two components which reveal completeley different physical behaviour are separated by a minimum around 15 kHz [4].

1.1.1 Radial properties

The integrated relative power of the fluctuation component below 15 kHz is about $\tilde{T}/T = 2\%$ (150 Hz–15 kHz). Its radial amplitude profile and radial propagation properties (Fig. 1), determined from the correlation of different radial channels, point to a diffusive propagating temperature disturbance. Its origin is located outside the observed radial range and it is propagating radially inward according to a heat diffusivity of $\chi_{inc} = 0.8$ m^2/s. A radial decay length of 2–3 cm (at 450 Hz) and a radial coherence length > 20 cm (*i.e.* infinite with respect to the radial range diagnosed) confirm its diffusive character. This is in perfect agreement with active temperature perturbation experiments where ECRH is modulated. The radial propagation of the fluctuation component around 40 kHz is completely different. Its phase velocity $2\pi f/k_r$ is directed outward

*Corresponding author's e-mail: hartfuss@ipp.mpg.de

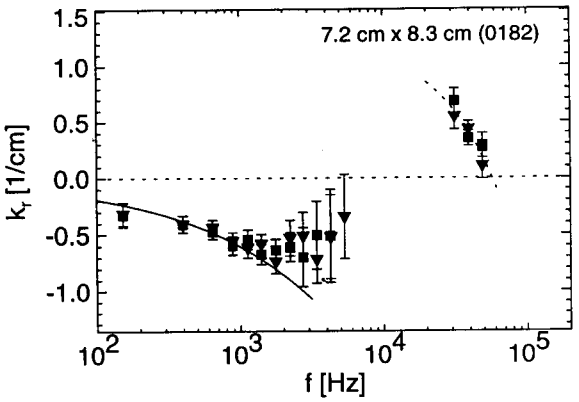

Fig. 1 Spectrum of the radial Wavenumber k_r.

(Fig. 1) with a dispersion relation which cannot be explained diffusively. Its coherence length (1.5–3 cm) is smaller than the observed radial region, pointing to a radial extended turbulence-like feature. Comparison of high-field-side and low-field-side measurements show an about 2 times larger fluctuation level on the low-field-side whereas the profile of the diffusive component is identical on both sides, *i.e.* it is constant on a flux-surfaces.

1.1.2 Correlation with Mirnov-coil signals

The integrated relative power of the component around 40 kHz which is believed to be the one relevant to turbulent driven transport, is about 0.6% on the high-field side. A clear coherence of 10–60% with a Mirnov-coil signal indicates corresponding magnetic field variations which are estimated to be in the order of some T/s. However, no mode-like spatio-temporal structure can be identified [1]. Correlation of density and temperature fluctuations have been found in a combined reflectometry-ECE experiment [3] and will be discussed in detail in a forthcoming paper.

1.1.3 Vanishing temperature gradient

As expected in a turbulent, convective picture, the temperature fluctuation component above 15 kHz disappears completely in the flat region of the temperature profile. Measurements with reflectometry show significant density fluctuations even in the $\nabla T=0$ region, indicating persistent plasma turbulence. According to the convective picture, the ∇T-dependence is separated and the "turbulence" $\tilde{A} = \tilde{T}/\partial_r T$ is investigated. The fluctuation component below 15 kHz is found in the $\nabla T=0$ region with a similar amplitude like in the finite-gradient region, as expected due to its diffusive nature.

1.1.4 Parameter scans

The dependence of the integral turbulence $\tilde{A}$ of the component above 15 kHz on parameters like ECR

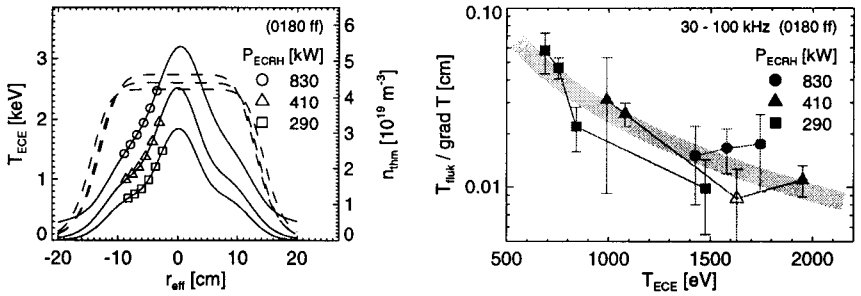

Fig. 2 ECRH power scan.

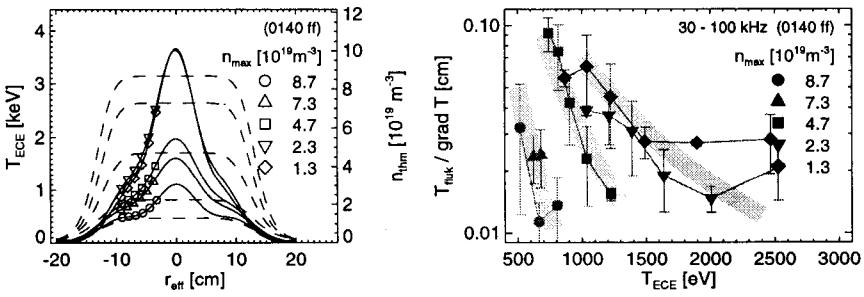

Fig. 3 Density scan.

heating power, plasma density, rotational transform ι and plasma current has been investigated. Earlier results [5] are correspondingly found looking at $\tilde{\Lambda}$. In the ι-scans discharges with poorest confinement show highest fluctuation or turbulence levels. An empirical attempt to assign local plasma parameters to the $\tilde{\Lambda}$-profiles points to an universal decrease of $\tilde{\Lambda} \propto T^{\alpha}$ with increasing temperature. In the case of the ECRH-powerscan (Fig. 2), an exponent $\alpha \approx -1.5$ has been found, whereas a similar analysis for the density scan yields different exponents ($\alpha = -2 ... -3.5$) for different densities (Fig. 3).

2. Non-Thermal Electron Distribution

2.1 Introduction

During ECRH heating at high power density, distortion of the Maxwellian electron distribution function is expected near the resonance zone with the creation of a suprathermal tail. In the simplest model a bi-Maxwellian distribution can be assumed consisting of a thermal and a suprathermal part. Whereas low field side ECE observation does not allow for unique interpretation (ambiguity between position and energy), by vertical observation the thermal emission is reduced to a relatively narrow frequency range because of the nearly constant magnetic field along the line of sight. The down-shifted radiation emitted by the suprathermal electrons is much less reabsorbed along the vertical path with a vertically viewing antenna system with Gaussian beam optics. It is arranged in a toroidal plane close ($\Delta\Phi \approx 5°$) to that where the ECRH is deposited. It is movable in radial direction, so it allows to localize the suprathermal electrons as the only diagnostic in the ECRH deposition plane. The non-thermal part of the emitted spectrum can be identified by comparison with numerical calculations and by investigation of the different time behaviour of the two components.

2.2 ECE spectra and numerical simulations

Low density plasmas heated by high power ECRH (400 kW and 800 kW, respectively, X-mode polarization) have been investigated. Fig. 4 shows a measured spectrum for the case of $P = 800$ kW, $n_{e0} = 1 \times 10^{19}$ m^{-3} and vertical observation (circles). A ray-tracing code is used to calculate ECE spectra including a suprathermal component. The ECE-spectrum is obtained by solving the radiative transfer equation along the ray path. Due to the presence of a local maximum of B along the viewing chord (close to the plasma centre) two peaks appear in the calculated ECE-spectrum (full line in Fig. 4) [2]. The maximum at higher frequencies comes from

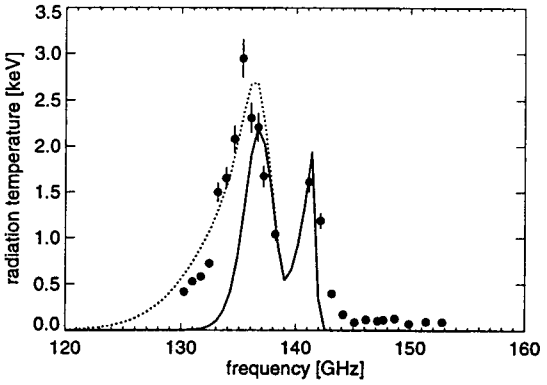

Fig. 4 Measurements *vs.* simulation.

radiation emitted by a region close to the plasma centre. Decreasing the frequency the thermal resonance moves to the plasma edge where the temperature is much lower. At frequencies below the minimum at 138–139 GHz the thermal resonance is shifted outside the plasma and only down-shifted emission is measured. Assuming a bi-Maxwellian distribution a good fit of the spectrum is possible (dotted line in Fig. 4). Spectra obtained by variation of plasma parameters are given in Fig. 5. Doubling the density leads to a strong decrease of the detected radiation temperature, although the central plasma temperature remains nearly unaffected. If the ECRH power is changed from 400 kW to 800 kW the low frequency peak increases and shifts to lower frequencies, as expected because of higher central temperature. By varying the radial position of the vertically viewing antenna it was found out that the radial extent of the spatial distribution of the

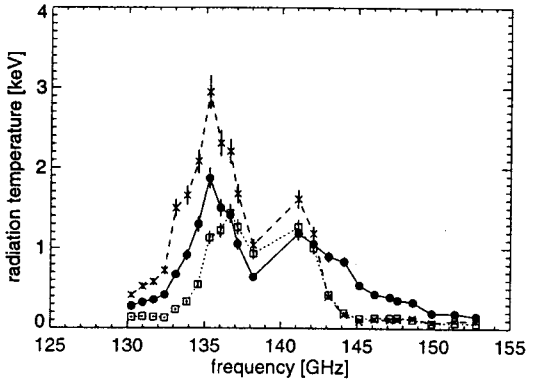

Fig. 5 ECE spectra measured with the vertically viewing antenna. (×) $n_{e0} = 1 \times 10^{19}$ m^{-3}, $P = 800$ kW; (●) $n_{e0} = 2 \times 10^{19}$ m^{-3}, $P = 800$ kW; (□) $n_{e0} = 1 \times 10^{19}$ m^{-3}, $P = 400$ kW.

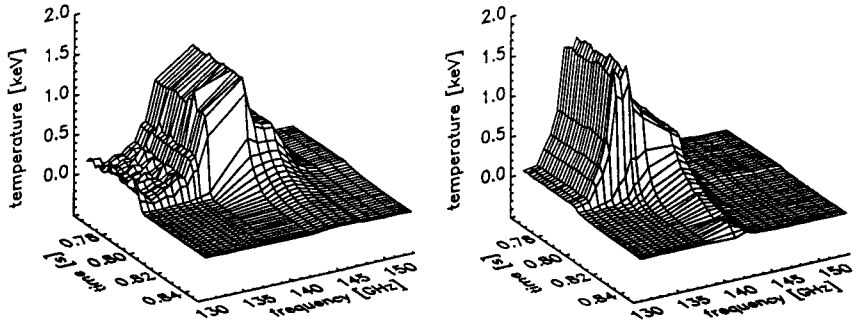

Fig. 6 Time behaviour of the ECE-spectrum after ECRH power switch-off. Left: "minimum B"; Right: "maximum B". No difference can be determined in the decay of the suprathermal radiation within the frame of measurement accuracy.

suprathermals is only about 2–3 cm, coinciding with the power deposition zone [6]. Calculations result in a strong dependence of the central density of the suprathermals $n_{e0}^{s.th.}$ on n_{e0} and P^{ECRH}, 0.5% n_{e0} ... $n_{e0}^{s.th.}$ ... 3% n_{e0}, whereas there is only a weak variation of $T_{\perp}^{s.th.}$ between 6 keV and 8.5 keV. Switch-off experiments give a further possibility to distinguish between the thermal and the suprathermal component of the spectrum [7]. The suprathermal radiation disappears on a time scale of about 1 ms which is attributed to the loss mechanism or at least to the collisional slowing-down. That shows the direct connection between ECRH power deposition and creation of suprathermal electrons.

2.3 Different magnetic configurations

At W7-AS the depth of the toroidal mirror of the magnetic field configuration can be changed. Measurements have been made in the so-called "minimum B" and "maximum B" configurations. In the latter a significantly smaller number of electrons in the ECRH launching plane is trapped. Fig. 6 shows the response of the ECE-emission after the switch-off of the ECRH for the two configurations. It is not possible to decide exactly the maximal radiation temperature in case of "minimum B" configuration because of the technically determined measurement gap between 138 and 141 GHz. But the "minimum B" configuration shows a larger amount of suprathermal electrons under otherwise same conditions (integration of suprathermal emission over the whole frequency range). This gives a hint that suprathermals are trapped in the local mirror, which leads to a higher particle density in the dynamic equilibrium of production, slowing down and drift. Besides Fig. 6 shows higher energies of the suprathermal in the "minimum B" configuration.

References

[1] M. Anton *et al.*, in these Proceedings, p.259 (1998).

[2] U. Gasparino *et al., Proc. of the 19th EPS Conf. on Contr. Fusion and Plasma Phys.* Innsbruck (1992) Vol II 1001.

[3] M. Häse, H.-J. Hartfuaß and M. Hirsch, *Correlation of Temperature and Density Fluctuations on W7-AS, 10th Joint Workshop on Electron Cyclotron Emission and Electron Cyclotron Resonance Heating*, Ameland, The Netherlands (1997) (Singapore: *World Scientific to be published*).

[4] H. J. Hartfuß, M. Häse, C. Watts, M. Hirsch, T. Geist and the W7-AS Team, Plasma Phys. Control. Fusion **38**, A227 (1996).

[5] H. J. Hartfuß, S. Sattler, M. Häse, T. Geist and W7-AS Team Fusion Engineering and Design **34-35**, 81 (1997).

[6] W. Pernreiter *et al., Non-thermal Electron Energy Distribution from Vertical ECE-Measurements at W7-AS Stellarator, Proc. 10th Joint Workshop on Electron Cyclotron Emission and Electron Cyclotron Resonance Heating*, Ameland, The Netherlands (1997) (Singapore: *World Scientific to be published*).

[7] M. Romé *et al.*, Plasma Phys. Control. Fusion **39**, 117 (1997).

[8] S. Sattler, H.J. Hartfuß and W7-AS Team, Phys. Rev. Lett. **72**, 653 (1994).

[9] C. Watts *et al.*, Phys. Plasmas **3**, 2013 (1996).